

University of California
Santa Barbara

The effects of magnetic fields, absorption, and relativity on the
polarization of accretion disks around supermassive black holes

A Dissertation submitted in partial fulfillment
of the requirements for the degree of

Doctor of Philosophy

in

Physics

by

Eric Agol

Committee in Charge:

Professor Omer Blaes, Chairperson

Professor Robert Antonucci

Professor Doug Eardley

August 1997

This dissertation of Eric Agol is approved

Doug Eardley

Robert Antonucci

Omer Blaes,
Committee Chairperson

June 1997

August 1997

Copyright by
Eric Agol
1997

ABSTRACT

The effects of magnetic fields, absorption, and relativity on the polarization of accretion disks around supermassive black holes

by
Eric Agol

Polarization of radiation emerging from accretion disks in active galactic nuclei (AGN) may be strongly affected by Faraday rotation, absorption opacity, and relativistic effects. We calculate the polarization of disk atmospheres including successively:

- 1) electron scattering with weak magnetic fields;
- 2) absorption opacity;
- 3) both magnetic fields and absorption opacity.

We then compute global disk models including relativistic effects.

We find the following results:

1) Faraday rotation by an equipartition magnetic field does not affect the polarization in the extreme ultraviolet, but depolarizes in the optical, which may help explain the low optical polarizations observed in QSO's.

2) Blueward of the Lyman edge, the polarization rises *above* the value expected from an electron scattering atmosphere. This arises because of the wavelength dependence of the absorption opacity combined with a source function in this region of the spectrum that has a steep variation with optical depth. We predict that the polarization should continue to rise blueward of the wavelength where the current observations end, that cooler spectra should be polarized more, and that the polarization angle should be parallel to the disk plane.

3) If absorption opacity dominates, then Faraday rotation generally has only a small effect on the emerging polarization because of the small electron column density along a photon mean free path. However, if the absorption opacity is not too large and it acts alone to increase the polarization, then the effects of Faraday rotation can be enhanced over those in a pure scattering atmosphere. Finally, while Faraday rotation often depolarizes the radiation field, it can in some cases *increase* the polarization when the thermal source function does not rise too steeply with optical depth.

4) Due to relativistic effects, the polarization rise blueward of the Lyman edge is reduced in magnitude and blueshifted for edge-on disks, while the polarization is small for face-on disks. This probably means that standard thin

accretion disks cannot explain the rise in polarization blueward of the Lyman edge seen in several quasars.

We also present spectropolarimetry of the broad H-alpha line in galaxy Arp 102B, and calculations of the polarization of stars during microlensing.

Contents

1	Introduction	1
1.1	History of quasars	1
1.2	What causes quasars to shine?	3
1.3	Why are quasars interesting?	6
1.4	Accretion disk problems	7
1.5	Overview	25
2	Effects of Faraday rotation	27
2.1	Introduction	27
2.2	Equations	29
2.3	Results	36
2.4	Polarization of magnetized disks	44
2.5	Conclusions	52
2.6	Appendix	58
3	Effects of absorption	63
3.1	Introduction	63
3.2	The atmosphere calculation	65
3.3	Results	66
3.4	Conclusions	76
3.5	Appendix A: grey atmosphere	77
3.6	Appendix B: complete linearization	78
4	Absorption and Faraday rotation	81
4.1	Introduction	81
4.2	Equations and numerical techniques	82
4.3	Constant q_ν atmospheres	83

4.4	Accretion disk polarization	98
4.5	Conclusions	104
5	Relativistic effects	109
5.1	Polarized transfer function	109
5.2	Equations	111
5.3	Imaging of an accretion disk	114
5.4	Polarization from accretion disks	116
5.5	Conclusions	125
5.6	Appendix	125
6	Polarization of Arp 102B	137
6.1	Introduction	137
6.2	Observations	139
6.3	Results	140
6.4	Discussion and conclusion	144
6.5	Acknowledgements	145
7	Polarization during microlensing	147
7.1	Introduction	147
7.2	Equations	149
7.3	Polarization during fold caustic crossing	150
7.4	Polarization during a binary lens event	154
7.5	Observational prospects	162
7.6	Caveats and conclusions	164
7.7	Acknowledgements	166
8	Conclusions	167
8.1	Acknowledgements	170

Chapter 1

Introduction to quasars and observational problems with accretion disk theory

1.1 History of quasars

By 1960, many sources in the Third Cambridge (3C) radio catalogue had been identified with low-redshift galaxies, such as 3C 295, starting a new class of astronomical objects now known as “radio galaxies.” However, there were also many unidentified 3C radio sources, i.e. with no visible counterparts. Mathews and Sandage (1963) photographed the regions near several radio sources which had good radio positions and found faint, point-like optical sources (assumed at the time to be stars) within 10 arcseconds of three of them, 3C 48, 3C 196, and 3C 286. All three optical ‘stars’ emitted most of their energy at short wavelengths (blue/ultraviolet) and did not have of the absorption lines associated with stars. Only one had an unidentifiable emission line.

In 1962, Hazard, Mackay, and Shimmins observed a fortuitous triple lunar occultation of another unidentified radio source, 3C 273, one of the strongest radio sources on the sky, with the Parkes radio telescope in Australia. The occultations allowed the position of the radio source to be pinpointed to $1''$, revealing that it was actually two sources $20''$ apart. One of the sources had an unusual flat spectrum (meaning it emits equal amount of energy per decade of frequency) and was smaller than the second source. Looking at a Palomar

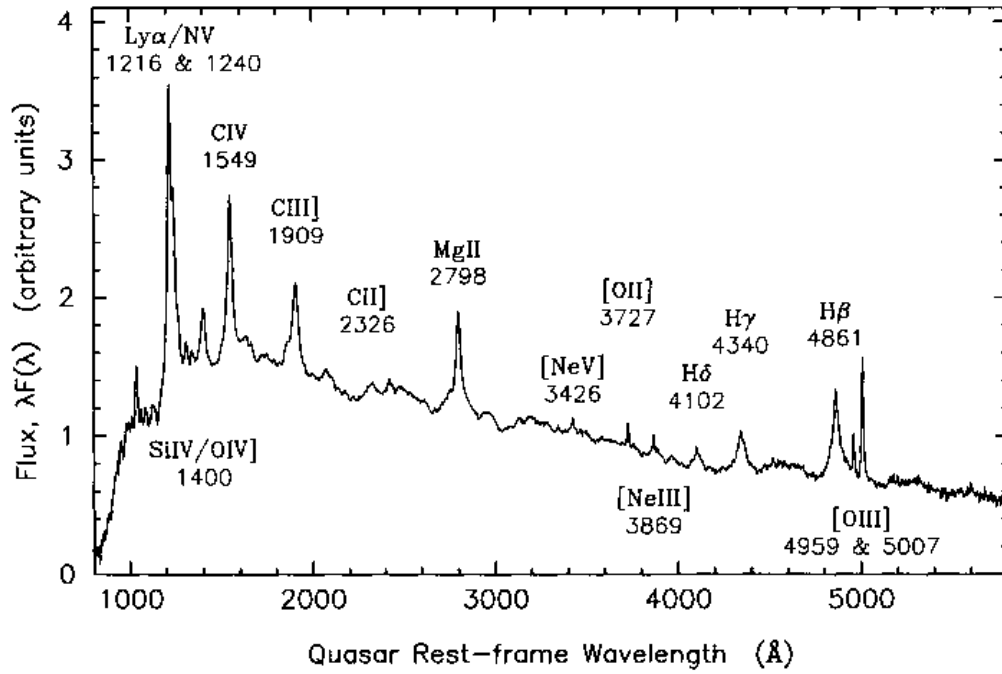


Figure 1.1: Composite quasar spectrum showing the various emission lines (from Francis et al. 1991).

plate revealed a ‘star’ at the position of the smaller, flat-spectrum source, and a wispy jet at the position of the larger source, making it the fourth identification of a radio star.

Maarten Schmidt (1963) took a spectrum of the 3C 273 source, and found several spectral lines which didn’t seem to correspond to any known atomic lines. Eventually he realized that the lines were redshifted by 15.8%, and when taking this into account, he identified hydrogen, oxygen, and magnesium emission lines, some rather broad. Assuming the redshift was cosmological, the luminosity would have to be about 100 times the luminosity of the entire Milky Way galaxy! This new class of objects discovered by Matthews, Sandage, and Schmidt were called ‘quasi-stellar optical sources with radio counterparts.’ To abbreviate this unwieldy name, Hong-Yee Chiu coined the term ‘quasar’ (Chiu 1965).

In the following years, more of the radio sources were identified with faint

blue ‘stars.’ Alan Sandage proposed that a puzzling class of blue stars, thought to be in our galaxy, might actually be quasars without a detected radio source. Sandage coined the term ‘quasi-stellar galaxies,’ or QSG’s, but currently the trend is to call them QSOs, for ‘quasi-stellar objects’ (although it is also common to use the term ‘quasar’ interchangeably for ‘QSO,’ despite the lack of radio detection). Sandage’s idea was confirmed when some QSGs were detected in the radio frequency, and thus were indistinguishable from quasars. Others still went undetected in the radio, and are now referred to as ‘radio-quiet quasars,’ (RQQs) somewhat of a contradiction in terms; quasars with detected radio emission are now called ‘radio-loud quasars.’ Most of the quasars now known have been discovered by looking in the optical for blue/ultraviolet pointlike sources; about 90% of quasars turn out to be radio quiet. Quasar spectra are characterized by broad emission lines ($\text{fwhm} \simeq 5,000 \text{ km/s}$), with a featureless continuum (see figure 1.1 for an averaged quasar spectrum). It also seems true that QSOs are the brightest form of active galactic nuclei, such as Seyfert galaxies, which have very similar spectral properties, but are not bright or distant enough to swamp the light of their host galaxy. Indeed, imaging with the Hubble Space Telescope has revealed that a large fraction of QSOs reside in galaxies. Radio-quiet quasars are the subject of this thesis: what causes them to shine?

1.2 What causes quasars to shine?

Soon after the discovery of quasars, it was soon realized that their redshifts were probably at cosmological distances ($> 100 \text{ Mpc}$). However, this meant that quasars were much brighter than any galaxy, yet they varied on timescales of years, making them impossible to be powered by normal stars. At the 1963 Texas Conference (Robinson et al. 1965), Hoyle and Fowler proposed that collapsing supermassive stars ($\sim 10^8 M_{\odot}$) might power the quasars through gravitational contraction. Some problems with this model are shedding angular momentum and preventing breakup of the star into smaller masses. At the same conference, John Wheeler proposed that matter falling onto a gravitational singularity at the center of a galaxy might be powering quasars. It was quickly argued that quasars were probably extragalactic due to their lack of proper motion and large redshift which was difficult to explain with the gravitational redshift of a stellar mass object.

In a seminal paper, Salpeter (1964) estimated the maximum amount of en-

ergy which could be released by Bondi-Hoyle accretion onto a black hole. Given the radius of the marginally stable circular orbit, about 5.7% of the rest mass energy of particles could be radiated away (Zel'dovitch and Novikov 1964 pointed out the same result for a collapsing supermassive star with matter orbiting it). He also pointed out that the Eddington luminosity limits the brightness of accreting black holes, and that the e-folding time for a black hole accreting at the Eddington rate is $\sim 10^8$ years. Salpeter envisioned massive black holes in the halo of our galaxy puncturing the disk and accreting matter as possibly leading to the QSO phenomenon.

Lynden-Bell proposed that QSOs are powered by ‘‘Schwarzschild throats’’ in the centers of galaxies which have larger than normal gas accretion rates into the center (Lynden-Bell 1969). He argued that every galaxy, if not every cluster, should contain a massive black hole, with a spectrum with a primary peak in the ultraviolet ($\sim 10^{15.5}$ Hz) and a secondary peak in the near IR ($\sim 10^{14}$ Hz) due to the inner parts of an accretion disk and reprocessing by dust on larger scales. Given that the area of the inner region of an accretion disk scales as the marginally stable circular orbit, and the luminosity of an accretion disk is limited by the Eddington luminosity, a simple estimate of the temperature of the emitting region is given by:

$$T_{eff} = 7 \times 10^4 \text{K} \left(\frac{L}{L_{edd}} \right)^{1/4} \left(\frac{M}{10^8 M_\odot} \right)^{-1/4}. \quad (1.1)$$

This corresponds to a peak energy of photon emission at 15 eV, which is as typically observed, implying that a supermassive black hole is needed to explain the energy peaking in the ultraviolet. This luminosity requires an accretion of matter at the rate of about $\sim 4 M_\odot/\text{yr}$ which is larger than the typical mass loss rate for an entire galaxy. Thus, a galaxy with an unusually large mass loss rate, such as would occur in starbursts or in colliding galaxies, may be necessary for feeding the quasars.

Hills (1975) proposed that tidal destruction of stars in galactic centers could feed a black hole, causing it to shine brightly, producing the quasar phenomenon. This model leads to several predictions that roughly agree with observations. The black hole should stop shining once the tidal radius equals the Schwarzschild radius, which occurs for a $M_{max} = 3 \times 10^8 M_\odot$ black hole (assuming stars of solar density are accreting). A black hole of this mass accreting at the Eddington limit corresponds to $\sim 10^{13} L_\odot$, about the maximum quasar luminosity

observed. A Schwarzschild black hole beginning at $10M_{\odot}$ should take about 2×10^9 years to reach this limit assuming $\eta = 0.3$, after which it would shut off, which corresponds to a Hubble time at about $z=2.8$ in an Einstein de Sitter universe. This might explain why there are fewer quasars seen at lower redshifts (Schmidt et al. 1991). Galactic centers with the largest stellar densities should then harbor supermassive black holes which went through a quasar phase, while lower stellar density galactic centers should harbor lower-mass, dimmer accreting black holes (the critical stellar density is about $1.5 \times 10^7 M_{\odot} / \text{pc}^{-3}$ for a black hole to grow to M_{max}). Later studies showed that if tidal disruption of stars by a supermassive black hole is important, then collisions of the stars will also lead to disruption, causing gas to feed in. In a recent review, Shlosman, Begelman, and Frank (1990) claim that feeding a black hole by star clusters requires too dense a cluster to be viable, and gas probably accretes from larger regions due to non-axisymmetric perturbations. Feeding by gas may also be needed to explain why some black holes can grow to greater than M_{max} .

Gas clouds orbiting the center of a galaxy have specific angular momentum $\sim 10^{29} \text{cm}^2 \text{s}^{-1} (r/1\text{kpc})(v/300\text{km/s})$. The maximum specific angular momentum of a particle near the horizon of a black hole is about $\sim 10^{24} M_8 \text{cm}^2 \text{s}^{-1}$. Thus, to accrete onto a black hole, the gas has to lose 99.999% of its angular momentum. This probably happens by dissipation processes such as collisions between clouds or transport of angular momentum through turbulence. Since the lowest energy configuration for a given angular momentum is a circular orbit, the gas is likely to form into a disk (since gas in circular orbits at different angles will collide and damp down into a disk). If the disk has a small mass relative to the black hole, the orbits will be Keplerian and there will be a large shear between adjacent orbits. Viscosity will cause heating and transport of angular momentum outward, causing gas to accrete onto the black hole, releasing a large fraction of its energy as electromagnetic radiation. This is the black hole model for the powering of quasars.

In the last two and a half decades, the black hole model for quasars has become the major paradigm. The success of the model relies mostly on theoretical arguments about the efficiency of accretion onto black holes. The observations, however, seem to be in contradiction to the detailed predictions of this model, and therein lies the motivation for this thesis.

1.3 Why are quasars interesting?

Since quasars are much brighter than galaxies, most of the furthest known objects in the Universe are quasars (the most distant quasar known has redshift 4.9, Schmidt et al. 1991). This makes them ideal tools for cosmology and high redshift astronomy (for a review of cosmological applications, see Shaver 1992). High redshift quasars are presumed to form in galaxies, and thus are tracers of large scale structure. If they were formed at the same time as galaxies, then the decrease in space-density of quasars for $z > 5$ indicates that the onset of galaxy formation occurred at about $z = 5$ (Shaver et al. 1996). Searches for companions to quasars have yielded many high redshift ‘primeval’ galaxies (Djorgovski, Pahre, Bechtold, and Elston 1996). Quasar light is absorbed by intervening gas, which has led to an industry of studying quasar absorption lines, leading to the discovery that galaxies cause the deepest quasar absorption lines (called ‘damped Lyman alpha systems’). As the absorption of quasar light is independent of the brightness of the absorbing objects, absorption line studies have led to a better understanding of the distribution of matter in the universe, such as the morphology of galaxies at high redshift (Lindner, von Alvensleben, and Fricke 1996). The highest known redshift cluster was discovered by looking at an absorption line system of a distant quasar (Giavalisco, Steidel, and Szalay 1994). One of the biggest impacts quasar absorption line studies have had is in measuring the primordial abundance of deuterium (Tytler, Fan, and Burles 1996). Also, measurement of the carbon fine structure absorption toward one quasar led to an estimate of the temperature of the cosmic microwave background at $z=1.8$ (Songaila 1996). The fine structure constant, α , proton gyromagnetic ratio, g_p , and ratio of electron to proton masses, m_e/m_p , can be constrained by measuring line frequency ratios in quasar absorption spectra (Cowie and Songaila 1995). The lack of continuous absorption of quasar light at energies above a Rydberg led to the realization that most of the intergalactic medium is ionized, the Gunn-Peterson effect (Gunn and Peterson 1965). A recent report of helium absorption toward one quasar may indicate that the intergalactic helium is not fully ionized (Jakobsen et al. 1994). A theoretical understanding of the spectrum of quasars would greatly aid in understanding absorption line data.

Since quasars are observed at large distances and are effectively point sources of light, they have a high probability of being gravitationally lensed. Multiply imaged quasars, which are the easiest to argue as being gravitationally lensed, can be measured for time delay(s) between the images. The time delay(s) com-

bined with a model of the gravitational lens object (usually a galaxy or cluster) yields a distance to the quasar independent of the distance ladder which is used to measure distances to galaxies (Refsdal 1964). This technique is being applied to several gravitationally lensed systems, and only recently has become accurate enough to compete with other methods of measuring distances (Kundic et al. 1997). Measuring the distance to a sample of gravitationally lensed quasars will eventually lead to estimations of the Hubble constant and deceleration constant which are as accurate as other methods such as supernovae or Sunyaev-Zeldovich effect. It is also hoped that quasars can eventually be used as cosmological candles. It has been shown that the luminosity of quasars anticorrelates with the equivalent width of certain emission lines (Baldwin 1977). If this effect can be calibrated at lower redshift, then possibly it can be used to measure cosmological parameters (Korista, Ferland, and Baldwin 1996). A theoretical understanding of how quasars are powered would greatly aid such studies.

Another tantalizing aspect of studying quasars is the prospect of testing general relativity. The profile of broad Fe K- α lines in several Seyfert galaxies has been attributed to fluorescent emission from a disk around a black hole, which is highly redshifted due to general relativistic effects (Tanaka et al. 1995). Higher luminosity (but more distant) QSOs have lower X-ray luminosities, but the optical/UV may be coming from near the horizon of the black hole. Thus, modeling of the emission region in QSOs may yield some understanding of strong field general relativity.

1.4 Problems with the standard thin accretion disk model

1.4.1 What is a “standard thin accretion disk”?

There are several crucial assumptions which simplify the calculation of spectra from accretion disks onto black holes. These assumptions lead to a model of the “standard thin accretion disk”:

- 1) *Geometrically thin disk.* This means that at all radii, $h/r \ll 1$, where h is the height of the surface of the disk and r is the distance from the center of the black hole. This allows modeling of the vertical gravitational acceleration

in cylindrical coordinates as:

$$g_z = \frac{GM_{BH}z}{(r^2 + z^2)^{\frac{3}{2}}} = \frac{GM_{BH}z}{r^3} + O((z/r)^2), \quad (1.2)$$

where M_{BH} is the mass of the black hole, G is the gravitational constant, and z is the distance from the equatorial plane. Since accretion with angular momentum is much more efficient than spherical accretion (Pringle, Rees, and Pacholczyk 1973), a thin disk leads to a much brighter luminosity than a spherically accreting flow for a given accretion rate.

2) *Alpha prescription.* If a disk of gas is on strictly Keplerian orbits, then it will not accrete since the molecular viscosity is too low by orders of magnitude for densities appropriate for accretion disks. Models of accretion disks posit a viscous force or friction between gas on adjacent orbits, which causes inner gas which is faster moving to exert an azimuthal force on gas exterior to it. This leads to heating and transport of angular momentum outwards, causing gas to accrete. The viscous force is given by

$$f_\phi = -t_{r\phi} = -\frac{3}{2}\eta\Omega \quad (1.3)$$

where f_ϕ is the force per unit area exerted in the ϕ direction by fluid elements at r on neighboring elements at $r+dr$, $t_{r\phi}$ is the viscous stress, η is the coefficient of dynamic viscosity ($\text{g cm}^{-1} \text{s}^{-1}$), and Ω is the Keplerian rotation frequency. It is not known what causes viscous dissipation in accretion disks, although plausible mechanisms are turbulent motions, chaotic magnetic fields, or a combination of both. To make progress in studying disks, Shakura and Sunyaev (1973) boldly made the assumption (based on dimensional analysis) that the viscous stress is proportional to the total pressure:

$$t_{r\phi} = \alpha P \quad (1.4)$$

where $\alpha < 1$ is a dimensionless parameter (Shakura and Sunyaev 1973) and P is the total thermal pressure.

If the viscosity is caused by turbulence within the disk, then η is given by $\eta = \rho v_{turb} \lambda_{turb}$, where v_{turb} is the velocity of turbulent eddies and λ_{turb} is the largest length scale of turbulent eddies. The scale of the largest eddies can't be more than the height of the disk, h , and the average velocity in the eddies can't be more than the speed of sound or else shocks will form, causing dissipation

which reduces the turbulent velocity. This leads to an upper limit $\eta < \rho c_s h$, which gives equation 1.4.

If viscosity is caused by magnetic fields, then $t_{r\phi}$ will be limited by the magnetic pressure. The magnetic field pressure cannot exceed the thermal pressure at the center of the disk, for if it does, a region with excess magnetic field becomes buoyant, causing it to escape from the disk. Thus, $t_{r\phi} \leq P_{mag} \leq P$, which gives the the same equation as 1.4. Sakimoto and Coroniti (1981) argue that the gas pressure limits the magnetic pressure, so that $t_{r\phi} = \alpha P_{gas}$ with $\alpha \leq 1$. This leads to a disk which is thermally stable and optically thick in the inner parts. The α parameterization of the viscous stress allows one to calculate the vertical structure of the disk. Usually α is assumed to be constant with radius; however, there is no reason to expect this would be the case.

3) *Optically thick disk.* This means that the effective optical depth $\tau_* \equiv \sqrt{3\tau_{abs}(\tau_{abs} + \tau_{es})} \gg 1$ at the disk midplane for all frequencies. This allows one to model the disk as an atmosphere with most of the flux coming from the bottom of the atmosphere, created in the optically thick regions inside the disk. This assumption is self-consistent in all but the innermost regions of the disk (if $t_{r\phi} = \alpha P_{tot}$). Shakura and Sunyaev (1973) give a formula for τ_* in the inner region of a disk around a Schwarzschild black hole which is radiation pressure and electron scattering dominated. There is a minimum in τ_* at $r = 10.8r_g$ at which point:

$$\tau_* = 0.26(\alpha/0.1)^{-17/16} M_8^{-1/16} (\dot{m}/0.3)^{-2}, \quad (1.5)$$

where τ_* is the Rosseland mean opacity of hydrogen. There are some problems with this expression since it assumes a one zone model for the disk, while the disk is much cooler and lower density at the surface than at the center. It neglects bound-free opacity which can be important for massive, cool disks. If the viscosity prescription is given as $t_{r\phi} = \alpha P_{gas}$, then τ_* becomes much greater than 1 (Sakimoto and Coroniti 1981). Thus, it is not clear if the optically thick assumption is appropriate for the inner regions of an accretion disk, and it will be important to calculate the entire vertical disk structure in future models.

4) *Stationarity.* If we assume that the structure of the disk does not change with time, then the accretion rate must be constant with radius in the disk. This gives the flux profile as a function of radius, independent of any assumptions about the viscosity source (Novikov and Thorne 1973; Page and Thorne 1974):

$$Q = \sigma T_{eff}^4 = \frac{3}{8\pi} \dot{M} \frac{GM}{r^3} \frac{Q}{\mathcal{BC}}^{1/2}, \quad (1.6)$$

where $\mathcal{B}, \mathcal{C}, \mathcal{Q}$ are relativistic factors defined in Novikov and Thorne (1973). When calculating accretion disk atmospheres, we will assume that the flux at the bottom of the atmosphere is given by equation 1.6.

5) *Equatorial plane.* The disk lies in the equatorial plane of the black hole for a rotating black hole. As the black hole accretes matter, it accretes the angular momentum of the matter at the last stable circular orbit. The timescale for a Schwarzschild black hole to spin up is roughly the amount of time it takes the black hole to double its mass from accretion. Thus, it is likely that AGN harbor rapidly spinning black holes (Bardeen 1970).

6) *Inner radius.* Usually the emission inside the last stable circular orbit, r_{ms} is ignored since gas falls inward with a large velocity, making the viscous stress quite small. The column density of gas inside r_{ms} is:

$$\Sigma = \frac{\dot{M}}{2\pi v_r r} = \frac{3\sqrt{3}r_g r_{ms} m_p L}{r\eta L_{edd}} \left(\frac{r_{ms}}{r} - 1\right)^{-\frac{3}{2}} \quad (1.7)$$

which gives $\Sigma \simeq 90\text{g/cm}^2(L/L_{edd})$ at $r = 3r_g$ for a Schwarzschild black hole independent of the mass of the black hole. Thus, the gas is optically thick to electron scattering inside the last stable circular orbit. However, the emission from this gas is negligible unless it reprocesses radiation created in other parts of the disk.

7) *Axisymmetry.* The disk structure is uniform in azimuth. This assumption is probably only valid for the time-averaged structure of the accretion disk (averaged over the orbital period of each radius). Non-axisymmetry will be very important to take into account for predictions of variability; however, it is currently too difficult to calculate.

Breaking any of these assumptions leads to complications which have been treated in various degrees of detail, and can lead to dramatic changes in the spectra and variability predictions for quasars. Most of the discussion in this thesis will be limited to bright radio quiet quasi-stellar objects (RQQs) since the radio and X-ray emission are much weaker than the optical/UV and they are less subject to variability due to relativistic beaming. The radio and X-rays are thought to be coming from a jet or corona, which if present would complicate interpretation of the emission coming from the putative accretion disk.

1.4.2 Spectral index problem

Given the above assumptions, there are various ways one can calculate the spectrum from an accretion disk. The most simple-minded method is to assume each annulus radiates as a blackbody, and sum the blackbodies over radius. Given the above effective temperature as a function of radius, the spectral index α in the optical/UV is $1/3$ ($f_\nu \propto \nu^\alpha$), as first pointed out by Lynden-Bell (1969). However, the median α 's in bright quasars are between -0.36 and 0 (Neugebauer et al. 1987; Francis et al. 1991; Cristiani and Vio 1990; Elvis et al. 1994; Zheng, Kriss, Telfer, Grimes, and Davidsen 1997). An averaged QSO spectrum is shown in figure 1.2. The optical/UV region has a slope which is close to being flat in νL_ν , while a simple accretion disk model predicts a slope of $4/3$. This disagreement we will refer to as the “spectral index problem.” Past attempts at fitting the quasar spectral index have included a mysterious power-law component that is usually attributed to synchrotron emission, and can account for some of the flux in the near infrared (Shields 1978; Sun and Malkan 1989). This power law component conveniently changes the spectral index in the optical/UV from $1/3$ to that observed. This may be valid in blazars, such as 3C 273; however, there is some evidence that most of the infrared emission comes from multi-temperature dust which cuts off abruptly at the dust sublimation temperature (1800 K for graphite), causing a dip in the flux at about 1 micron (Rees et al. 1969; Berriman 1990; Barvainis 1993). The dust is probably absorbing light from the central engine and radiating in the infrared, since its flux is larger than the gravitational energy released at large radius where it must exist to stay cool (Sanders et al. 1989). But, if the infrared bump is due to dust, and a synchrotron power law is not present, then the optical/UV slope is incorrect. Antonucci and Barvainis (1988) suggest that the “Big Blue Bump” (BBB) could be due to optically thin free-free emission, which predicts the correct optical/UV slope without an ad-hoc power law, but probably has trouble producing the large luminosities seen in quasars since optically thick emission is more efficient at radiating (see also Barvainis 1993; Ferland, Korista, and Peterson 1990).

Another problem is that accretion disks cannot explain the X-ray region of the spectrum (see figure 1.2). This problem is worse in Seyfert galaxies, where the X-rays can contain a comparable amount of power as the BBB. It is possible that a weak corona exists above the accretion disks in bright QSOs, which Compton-scatters photons from the disk, leading to a soft X-ray power

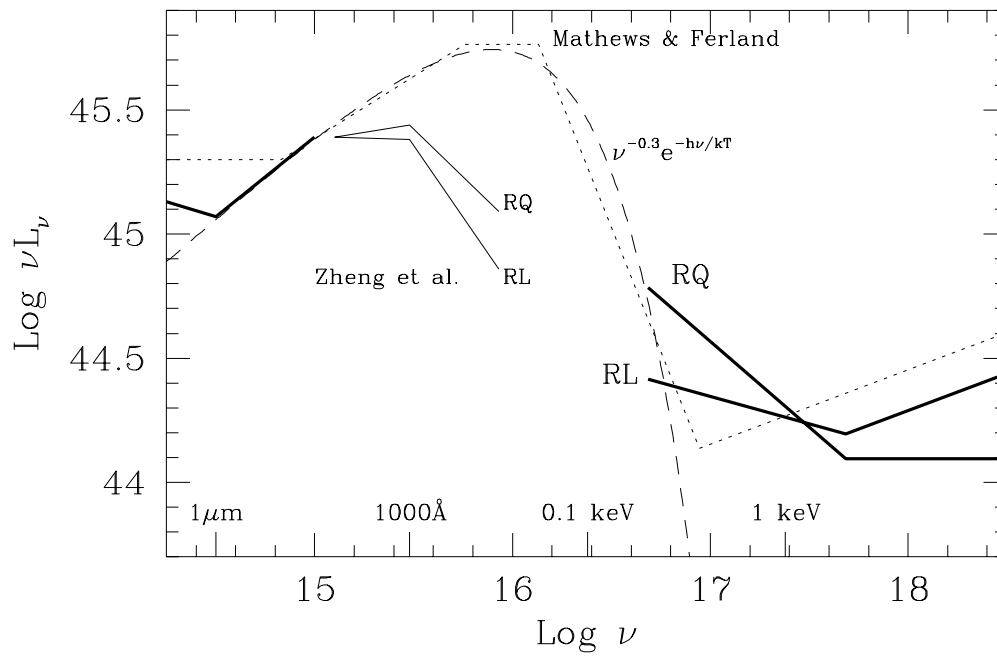


Figure 1.2: Spectral energy distribution from Laor, Fiore, Elvis, Wilkes, and McDowell (1997).

law, consistent with the observations (Zheng et al. 1997). However, the X-rays could also be produced in a jet or in localized flares.

One possible modification of the thin disk is that irradiation of the outer parts of the disk by the inner parts causes reemission of energy at larger radii, leading to a flatter temperature profile, which agrees better with the observed spectral indices. Irradiation of the outer parts of the disk by the inner parts can occur if the inner disk flares or if the disk is warped by Lens-Thirring precession (Bardeen and Petterson 1975) or radiation instability (Pringle 1996).

An intriguing possibility is that quasars are accretion disks in an outburst phase, much like dwarf novae, caused by a thermal-viscous instability (Siemiginowska et al. 1996). Since the disk is not stationary, the effective temperature can be much different than that in a stationary disk, leading to a spectral slope which agrees much better with the observations for certain choices of α in the hot and cool states. This model implies an outburst duty cycle of about 10% with a period of about 10^6 years, which may cause a problem for the model since luminous radio lobe selected objects all have BBBs, and since the lobes last as long as 10^8 years, this implies that the duty cycle is 100% over a 10^8 year period (Ski Antonucci, private communication).

Instead of assuming the radiation is a blackbody, a more elaborate way to calculate the spectrum emerging from a disk is to treat the surface of the disk as a stellar atmosphere, with a gravitational acceleration calculated from the disk scale height. This assumes 1) the disk is optically thick; 2) no flux is created within the atmosphere region so the radiation emerging from the bottom of the atmosphere can be treated in the diffusion approximation; 3) the scale height of the atmosphere is much less than the disk scale height, so the gravitational acceleration is approximately constant. These assumptions aren't perfect approximations, but give more accurate theoretical predictions than the blackbody assumption (Hubeny and Hubeny 1997). Several papers have calculated stellar atmospheres for disks at varying levels of sophistication (Czerny and Elvis 1987; Laor and Netzer 1989; Sun and Malkan 1989; Störzer, Hauschildt, and Allard 1994; Coleman 1993). Figure 1.3 shows a cartoon of a disk atmosphere. The atmosphere is assumed to be locally plane-parallel and the gravitational acceleration (assumed to be constant within the atmosphere) is opposed by a pressure gradient. The flux at the bottom of the atmosphere is assumed to be a blackbody, and the goal of the atmosphere calculation is to find the emergent spectrum, f_ν .

The next most detailed way to calculate the spectrum emerging from a disk

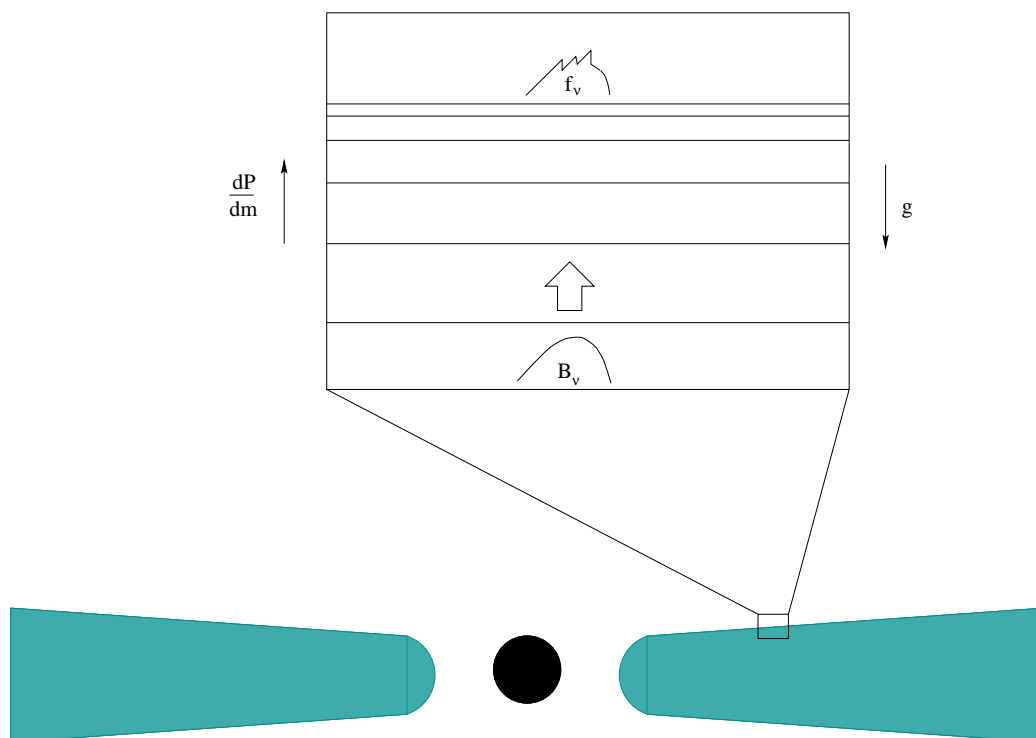


Figure 1.3: Schematic of accretion disk around black hole. The zoomed area represents the accretion disk atmosphere

is to extend the atmosphere to the disk center, including the changing gravitational acceleration as a function of height and the dissipation of energy. The uncertainty of the disk viscosity mechanism makes this somewhat dubious, although Hubeny and Hubeny (1997) claim that the spectra are insensitive to the viscosity prescription used. The most complete method for computing the spectrum will be to do the two dimensional radiative transfer, including the effects of self-irradiation. This should be coupled with global magnetohydrodynamical simulations of the disk, which must await huge advances in computing power and a much better understanding of the viscosity mechanism.

1.4.3 Lyman edge problem

Yet another problem with accretion disk models is the lack of a feature in total flux at the Lyman edge (Smith et al. 1981; Antonucci, Kinney, and Ford 1989; Koratkar, Kinney, and Bohlin 1992a). This causes a problem for both optically thick and thin models if the temperature of the emission region is less than about 10^5K , when hydrogen bound-free opacity is significant. In the context of standard thin accretion disks, Kolykhalov and Sunyaev (1984) calculated the spectrum of a thin accretion disk using the LTE atmospheres of Kurucz (1979). They concluded that typical QSOs should have huge Lyman absorption edges, broadened by Doppler effects. However, the absorption edge is increased by assuming LTE and surface gravities appropriate for stars, rather than accretion disks. The Lyman edge is reduced by using a lower gravitational acceleration appropriate for accretion disks (Coleman 1993) and including non-LTE effects (Störzer et al. 1994). If a hot layer exists above the disk, the Lyman edge can be reduced by Compton scattering of lower energy photons to ‘fill in’ the deficit of flux blueward of the edge (Czerny and Zbyszewska 1991; Lee, Kriss, and Davidsen 1992). Relativistic effects can in certain circumstances broaden any intrinsic edge enough to render it undetectable (Laor 1992). There does appear to be a spectral break around 1000\AA in averaged quasar spectra (Zheng et al. 1997), which may be attributed to Compton scattering of a redshifted Lyman absorption edge by an extended corona (see figure 1.4). This can also account for the soft X-ray properties of radio-quiet QSOs (Laor et al. 1997). Barvainis (1993) points out that optically thin, high temperature emitting gas has a rather weak Lyman emission edge; however, a small emission edge is still present and would need to be smeared (by relativistic effects or Comptonization) to agree with the lack of observed Lyman features in real QSOs.

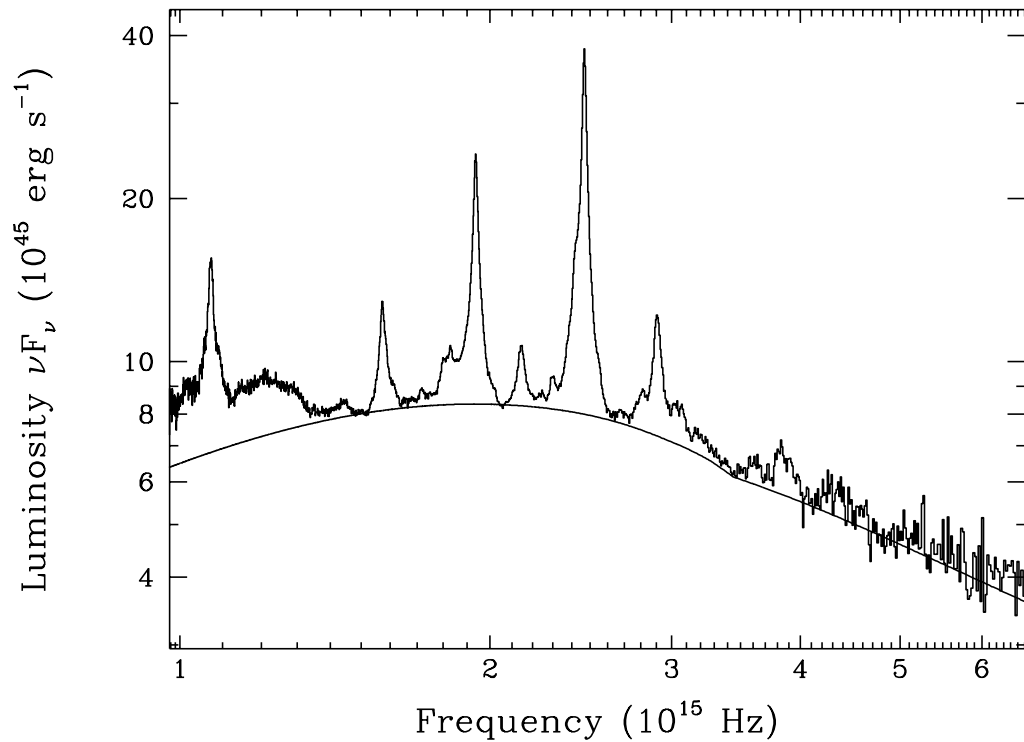


Figure 1.4: Averaged QSO spectrum (from Zheng, Kriss, Telfer, Grimes, and Davidsen 1997). The solid line is a model of an accretion disk with a black-body spectrum, multiplied by $\exp -(\nu/\nu_0)^3$ for $\nu > \nu_0 = 13.6\text{eV}/h$, and then Comptonized by a spherical corona of Compton optical depth = 1 to mimic a Comptonized Lyman edge.

1.4.4 Polarization problems

If electron scattering dominates the opacity in AGN accretion disk atmospheres, then the polarization can be as large as 11.7% (Rees 1975; Chandrasekhar 1960). Figure 1.5 shows the polarization from a plane-parallel atmosphere as a function of $\cos i$ where i is the inclination angle measured from the vertical. Optical observations of luminous QSOs do not reveal polarizations as high as expected (Berriman et al. 1990). However, we may be preferentially viewing the bright quasars more face-on due to obscuration by a torus in the equatorial plane (Antonucci 1984), thus the polarization is reduced. The sample of Berriman et al. (1990) shows a maximum polarization of 2.5%. This corresponds to a viewing angle of 60° from face-on if the emission is coming from an electron-scattering dominated disk. Figure 1.6 shows the number distribution of quasars with a given polarization, assuming an electron-scattering dominated disk viewed at an angle of less than 60° , compared to a histogram of the data from Berriman et al. (1990).¹ Note that there is a deficit of objects with high polarizations. In objects where a jet is observed, the polarization angle tends to align with the jet structure (Stockman et al. 1984). If the polarization is due to electron scattering in an optically thick disk, we would expect the polarization to be perpendicular to the axis of symmetry (assumed to be parallel to the jet axis), so this model is clearly wrong. This may indicate that the polarization is not due to electron scattering in the atmosphere of the disk, or that the scattering geometry is not plane parallel, e.g. a rough disk surface or a geometrically thick disk with a funnel (Coleman and Shields 1990; Kartje and Königl 1991). The position angle may also change if the disk is optically thin (Phillips and Mészáros 1986). In objects which have been observed at different wavelengths, the polarization tends to rise toward shorter wavelengths, which is also at odds with the wavelength independence electron scattering. It may be that much of the observed continuum polarization does not originate in the putative accretion disk at all, but occurs because of reprocessing on larger scales (e.g. Königl and Kartje 1994). If the direct continuum is unpolarized, the observed polarization may be caused by scattering by gas and dust on a larger scale. Scattering by dust in a torus or outflow can cause polarization which is low and parallel to the disk axis for near face-on orientation, while the polarization is high and perpendicular to the accretion disk axis for high inclination angles (Kartje

¹Blazars are excluded from this plot since they have non-thermal (i.e. featureless power law) spectra which are highly polarized, probably due to synchrotron radiation.

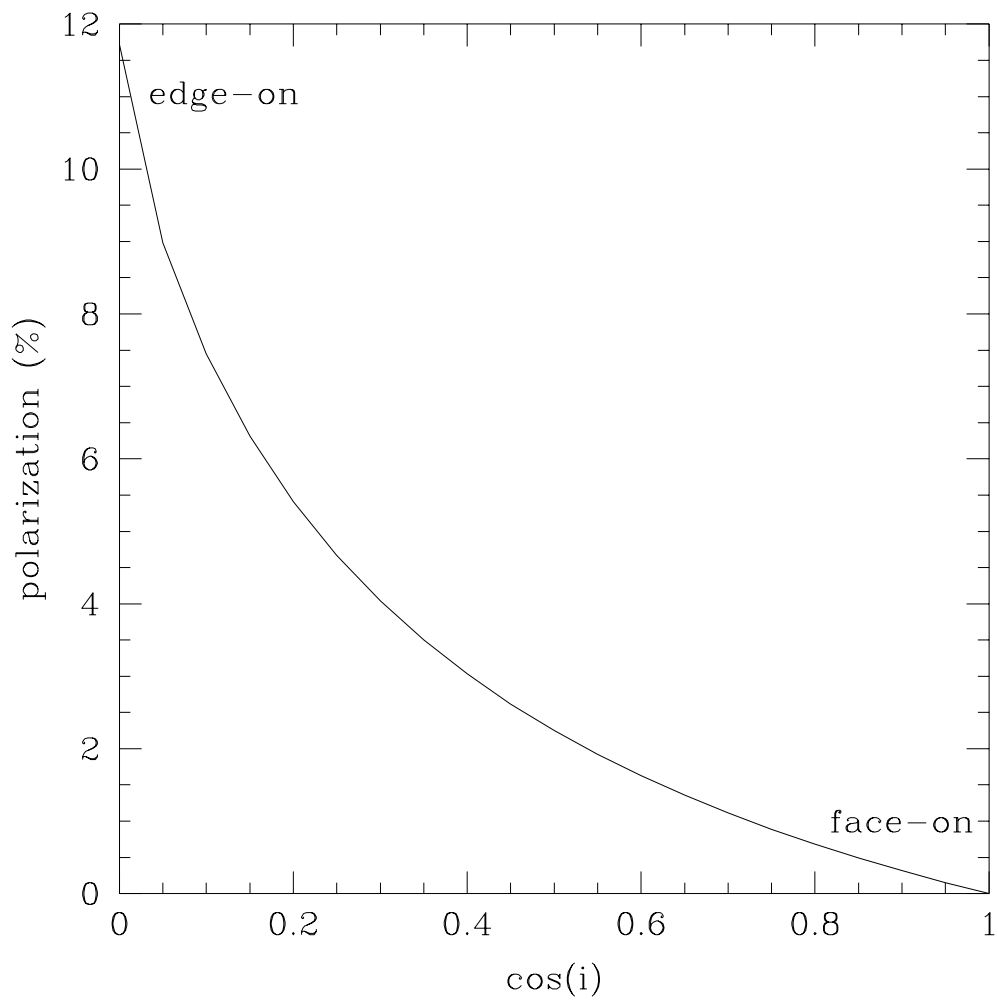


Figure 1.5: Polarization from a semi-infinite electron scattering atmosphere.

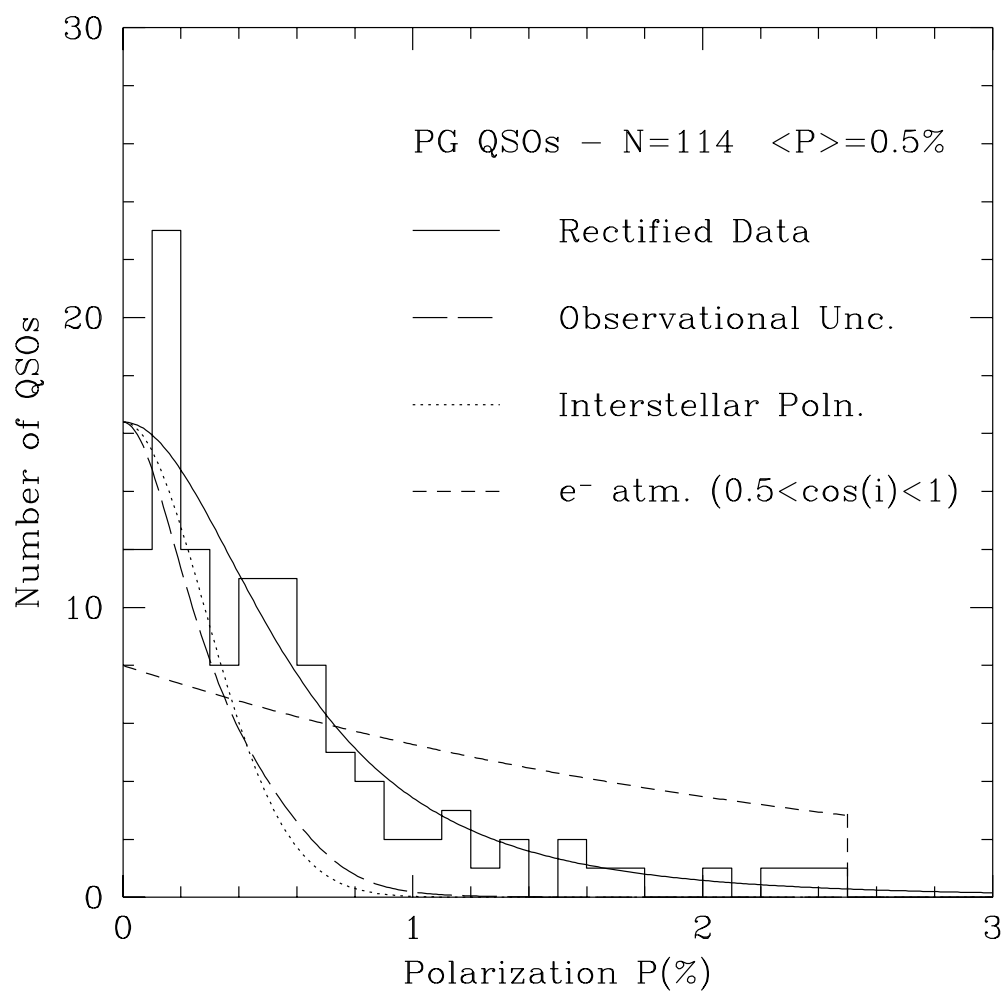


Figure 1.6: Polarization in R-Band of Palomar Green optically selected, non-blazar QSOs, compared with the expectation of an electron scattering atmosphere. (Figure taken from Berriman et al. 1990.)

1995).

Absorption opacity and relativistic effects in the standard disk can reduce the degree of polarization and produce a rotation of the position angle at high frequencies (Laor, Netzer, and Piran 1990, hereafter LNP). Moreover, these authors predict that the polarization should drop blueward of the Lyman edge and the polarization angle should rotate at short wavelengths. This signature should be more robust than that of a Lyman edge in total flux since there is intrinsically higher contrast across the edge in polarization over more parameter space. Also, foreground HI absorption should not affect the percent polarization, though it may affect the total flux. However, polarization observations require a higher signal to noise ratio if the polarized flux is low, as is the usual case for RQQs. To test LNP's prediction, two groups observed several QSOs with the Faint Object Spectrograph on the Hubble Space Telescope to look for polarization near the Lyman edge. To their surprise, several QSOs showed a *rise* in polarization blueward of the Lyman edge. The data are shown in figures 1.7-1.9. Further ground-based spectropolarimetry of $z > 3$ QSOs has not revealed a polarization rise blueward of the Lyman edge (Antonucci, Geller, Goodrich, and Miller 1996); however, higher redshift QSOs are more subject to foreground absorption, which makes high signal-to-noise observations more difficult. Three QSOs observed at Lick Observatory by Antonucci et al. (1996) are consistent with zero polarization blueward of the Lyman edge, and low or zero polarization redward.

1.4.5 Variability problems

Not much is known about the variability of radio quiet QSOs. Cutri et al. (1985) have observed that QSOs are more variable at shorter wavelengths, and not variable in the infrared. The spectral indices between $10^{14} - 10^{15} Hz$ tend to be flatter when the QSO brightens, and the optical/ultraviolet vary in phase (i.e. the amplitude of the variability in the ultraviolet is larger). If the emission is optically thick, an increase in temperature would cause the observed wavelength range to be on the Rayleigh-Jeans part of the spectrum rather than the peak of the blackbody, making the spectrum harder (i.e. flatter). If the emission region is single-temperature optically thin emission, then an increase in temperature also leads to a flatter spectral index as observed (Barvainis 1993). Alternatively, the variable part may have a flat spectral index due to hot optically thin free-free emission.

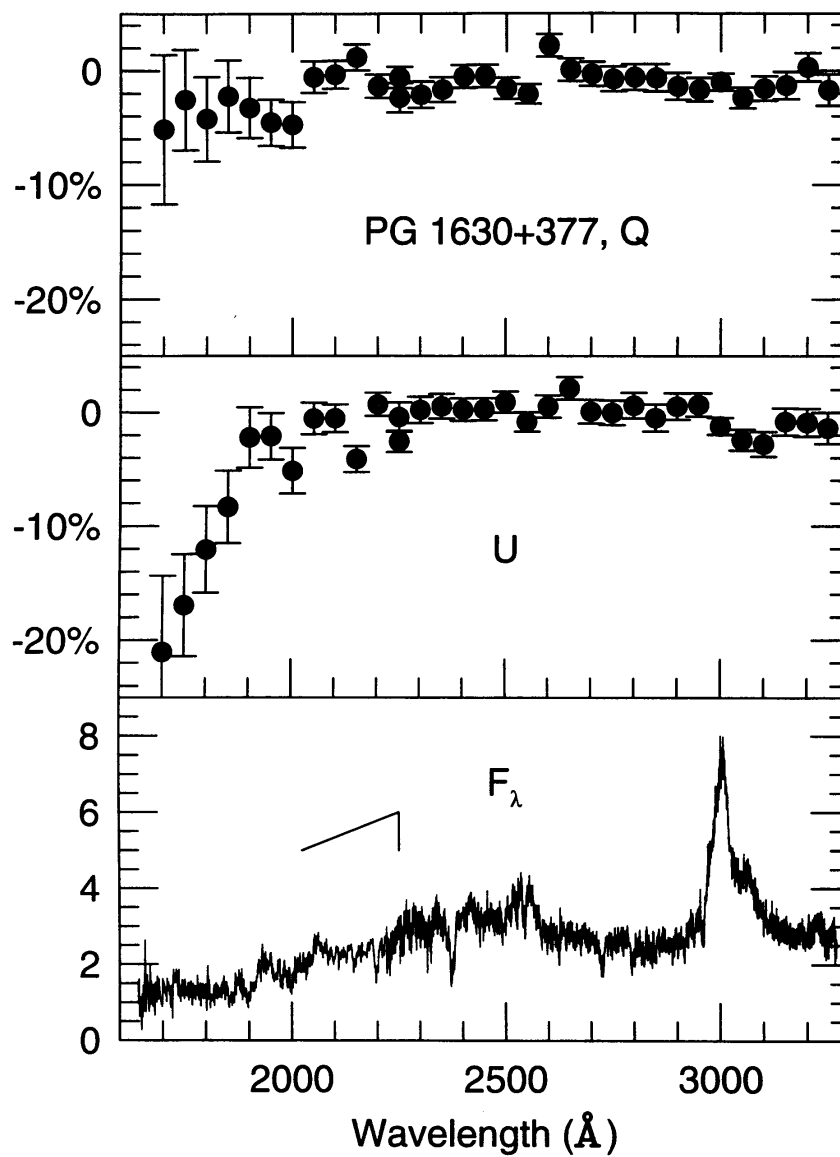


Figure 1.7: Polarization of QSO PG 1630+377 in observed frame (from Koratkar, Antonucci, Goodrich, Bushouse, and Kinney 1995).

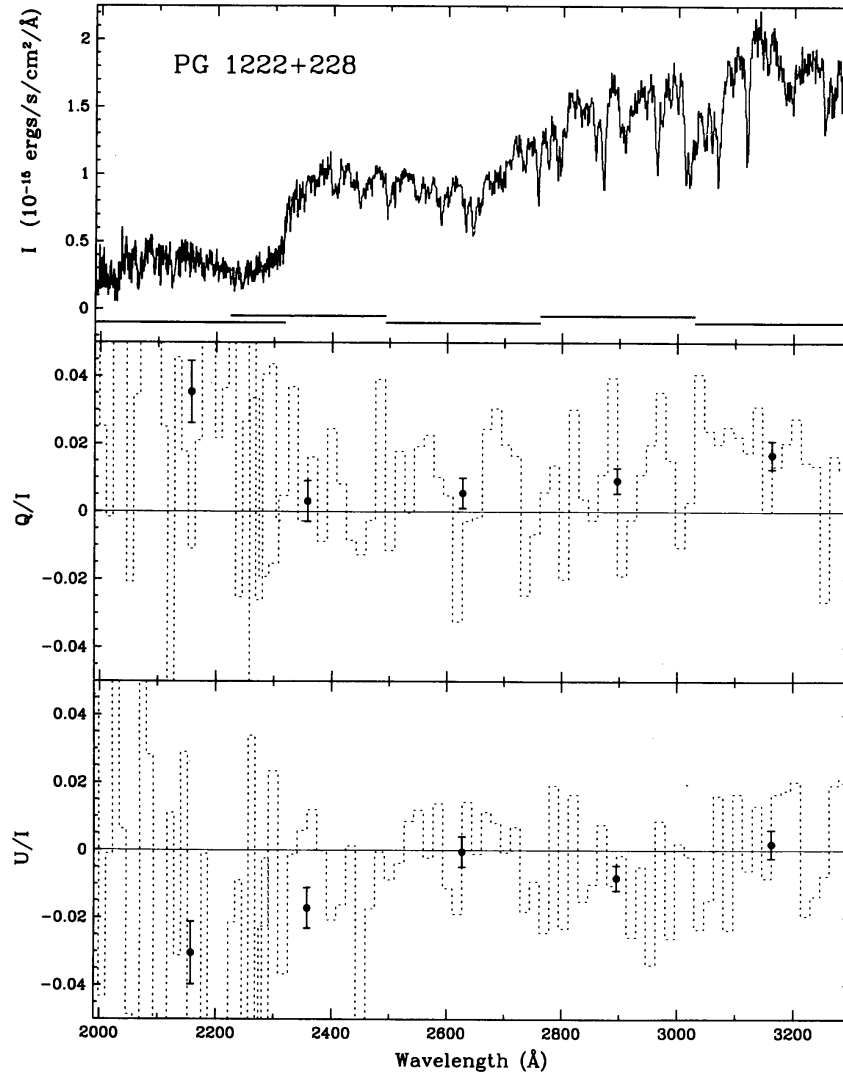


Figure 1.8: Polarization of QSO PG 1222+228 in observed frame (from Impey, Malkan, Webb, and Petry 1995).

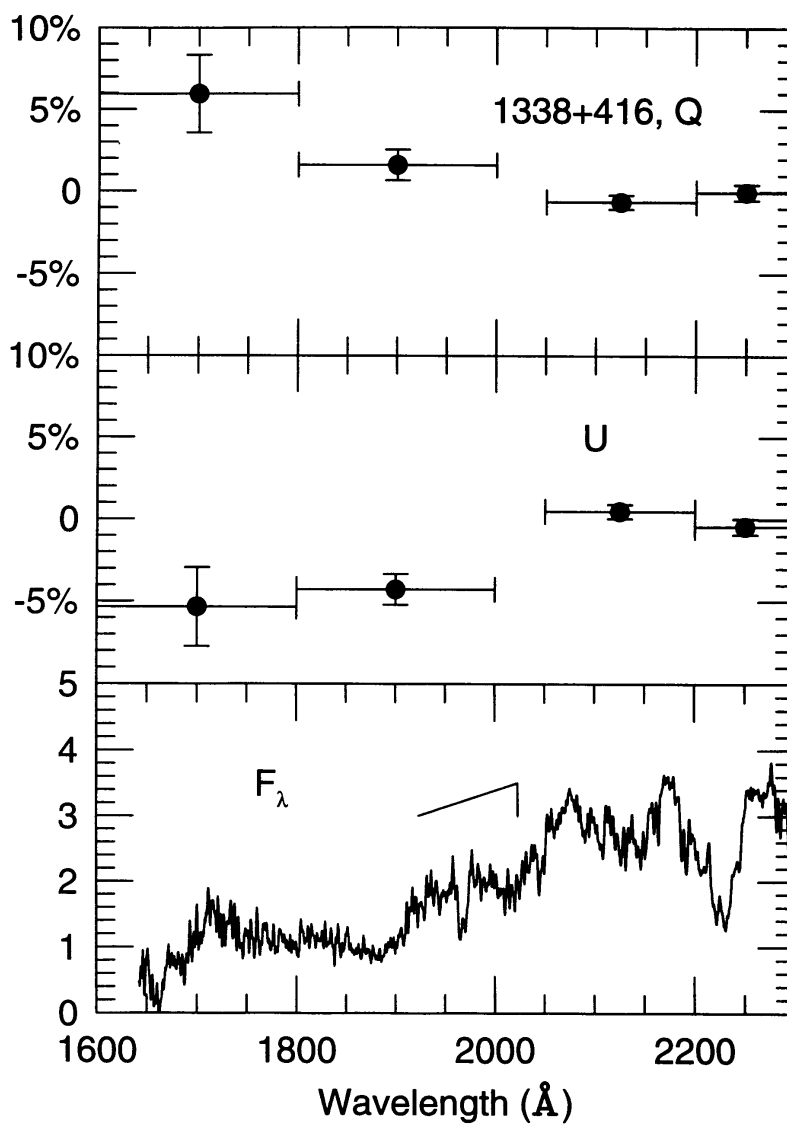


Figure 1.9: Polarization of QSO PG 1338+416 in observed frame (from Koratkar, Antonucci, Goodrich, Bushouse, and Kinney 1995).

In the simplest version of a steady accretion disk, the variability is caused by changes in the accretion rate in the outer regions, and thus the timescale for variability is $t_{visc} \sim r/v_r \sim 2 \times 10^5 \text{yr} \alpha_{0.1}^{-0.8} \dot{M}^{-0.3} M_8^{-.25} r_{16}^{1.25} f^{1.2}$ (Siemiginowska, Czerny, and Kostyunin 1996; Lightman 1974a). However, instabilities are likely to cause non-axisymmetric perturbations in an accretion disk, leading to short term time variability. These perturbations will be diluted in amplitude and limited by the timescale for shearing of localized regions (Pringle 1981), given by

$$t_{shear} = \frac{\Omega^{-1} R}{\Delta R} = 1 \text{yr} M_9^{-1/2} R_{15.5}^{3/2} \epsilon_{0.1} \quad (1.8)$$

where $\epsilon_{0.1} = 10\Delta R/R$, M_9 is the black hole mass in terms of $10^9 M_\odot$, and $R_{15.5} = R/10^{15.5} \text{cm}$, chosen to be roughly the radius of maximum flux for a $M_9 = 1$ black hole. Since perturbations will be smoothed out on timescales longer than t_{shear} , this is the longest timescale on which non-azimuthal fluctuations can exist, which is consistent with the current observations of high luminosity QSOs. Thermal-viscous instabilities can cause the disk to become corrugated in radius, and as the low density parts become optically thin they cool inefficiently and heat up, making the disk thick (Lightman and Eardley 1974; Lightman 1974a; Lightman 1974b). The viscous timescale for such variations is quite long, however. Rapid variability can be caused by magnetic flares which cause hot spots or lensing of hotter regions of the disk as they pass behind the black hole.

1.4.6 Microlensing constraints

Observations of the Einstein Cross have revealed flux variations in the individual images which have been attributed to microlensing by stars in the lens galaxy (Irwin et al. 1989). The sharpness of the detected variations (25% in 26 days for image A, Racine 1992) implies a maximum source size of about $2 \times 10^{15} \text{cm}$ (Wambsganss, Paczyński, and Schneider 1990). Making some assumptions about the amplification, cosmological parameters, and lens mass distribution, the brightness temperature is constrained to be greater than $3 \times 10^5 K$ (Rauch and Blandford 1991). Rauch and Blandford (1991) claim that this rules out an optically thick emission region as the source: a thin accretion disk with a radial temperature profile chosen to agree with the Einstein Cross spectral slope is too large to be consistent with the microlensing observations. However, arbitrary modifications of the standard disk are marginally consistent with the

microlensing size constraint (Jaroszyński, Wambsganss, and Paczyński 1992). A single, optically thin cloud is too large to be consistent with the microlensing constraint; however, a large number of optically thin cloudlets, an irradiated disk, or a disk surrounded by a sphere of optically thin cloudlets can be constructed to be marginally consistent with the microlensing size constraint and observed spectral index (Czerny, Jaroszyński, and Czerny 1994; Jaroszyński and Marck 1994). Future observations of the spectral or color changes during sharp amplification events will be able to distinguish between these various models (Wambsganss and Paczyński 1991).

1.5 Overview

In this thesis, we consider the problem of polarized radiative transfer in accretion disk atmospheres to confront the polarization conflicts addressed above. Magnetic fields are probably present in accretion disks, and can destroy polarization in the optical and near UV by Faraday depolarization. Chapter 2 addresses polarized radiative transfer in a scattering atmosphere including Faraday rotation by magnetic fields. Absorption opacity can play a role in reducing or enhancing polarization compared to that in a scattering atmosphere. Chapter 3 presents calculations of polarized radiative transfer in stellar atmospheres with parameters appropriate for accretion disks, including absorption opacity. The interplay between Faraday rotation and absorption opacity can lead to new effects, which are presented in chapter 4. When calculating the polarization emerging from an accretion disk around a black hole, the effects of special and general relativity must be included. In chapter 5 we present a fast and accurate method to calculate the polarization coming from an accretion disk around a black hole, and combine this with our atmosphere calculations. The final chapters are published papers related to polarization from QSOs: chapter 6 presents spectropolarimetry results from observations of Arp 102B, and chapter 7 presents a calculation of the polarization of a star during microlensing by a binary lens.

